iScience

CellPress
OPEN ACCESS

Article

Climate warming triggers the emergence of native viruses in Iberian amphibians

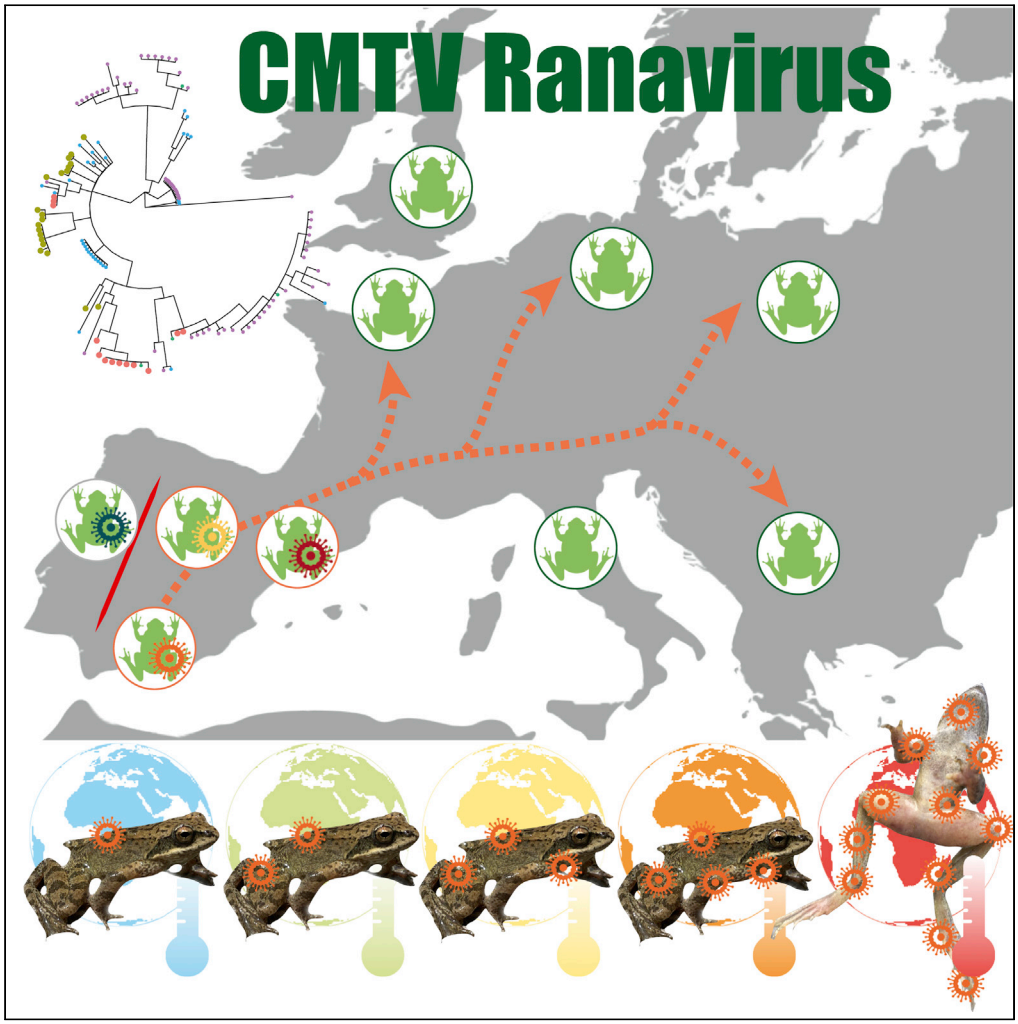

Barbora Thumsová, Stephen J. Price, Victoria González-Cascón, ..., Gonçalo M. Rosa, Annie Machordom, Jaime Bosch

jaime.bosch@csic.es

Highlights

The Iberian Peninsula is a hotspot for Ranavirus diversity, particularly CMTV

Ranaviruses are linked to mass mortalities in Iberia at least since the 1980s

Wide diversity among CMTVs in Europe is consistent with spread by natural dispersal

CMTV outbreaks are triggered by ongoing climate warming

Thumsová et al., iScience ■■, 105541 ■■, 2022 © 2022 The Author(s).
https://doi.org/10.1016/j.isci.2022.105541

Please cite this article in press as: Thumsová et al., Climate warming triggers the emergence of native viruses in Iberian amphibians, iScience (2022), https://doi.org/10.1016/j.isci.2022.105541

iScience

CellPress
OPEN ACCESS

Article

Climate warming triggers the emergence of native viruses in Iberian amphibians

Barbora Thumsová,[1,2] Stephen J. Price,[3] Victoria González-Cascón,[2] Judit Vörös,[4,5] Albert Martínez-Silvestre,[6] Gonçalo M. Rosa,[7,8] Annie Machordom,[2] and Jaime Bosch[9,10,*]

SUMMARY

The number of epizootics in amphibian populations caused by viruses of the genus *Ranavirus* is increasing worldwide. Yet, causes for pathogen emergence are poorly understood. Here, we confirmed that the *Common midwife toad virus* (CMTV) and *Frog virus 3* (FV3) are responsible for mass mortalities in Iberia since the late 1980s. Our results illustrate the Iberian Peninsula as a diversity hotspot for the highly virulent CMTV. Although this pattern of diversity in Europe is consistent with spread by natural dispersal, the exact origin of the emergence of CMTV remains uncertain. Nevertheless, our data allow hypothesizing that the Iberian Peninsula might harbor the ancestral population of CMTVs that could have spread into the rest of Europe. In addition, we found that climate warming could be triggering the CMTV outbreaks, supporting its endemic status in the Iberian Peninsula.

INTRODUCTION

Emerging infectious diseases are important drivers of amphibian population declines and species extinctions worldwide, including the Iberian Peninsula.[1,2] The vast majority of mortality events in that area were associated with chytridiomycosis, a disease produced by the amphibian chytrid fungus *Batrachochytrium dendrobatidis*.[3–5] However, the first die-off episodes were recorded earlier in 1992 in the Spanish Pyrenees, where the causative agent of the overt signs of disease remained unresolved.[6] Similar signs were later observed over 400 km west in 2005, which was thought to be the first mass mortality event attributed to ranaviruses.[1]

Ranaviruses (family Iridoviridae) are large, double-stranded DNA viruses capable of infecting fish, reptiles and amphibians.[7,8] These pathogens were first isolated from Northern leopard frogs (*Lithobates pipiens*) in the US in the 1960s.[9] Amphibian-associated ranaviruses have been categorized into three main groups namely *Frog virus 3* (FV3)-like, *Common midwife toad virus* (CMTV)-like, and *Ambystoma tigrinum virus* (ATV)-like viruses.[10] Internationally, strains from all three major groups have been described as the cause of mass mortalities and morbidity.[8] Although the highly virulent CMTV-like viruses show the most restricted range, they are the most common ranaviruses in continental Europe. Outside of Europe, the presence of CMTVs has never been described in wild populations.[11,12]

The growing number of reports of Ranavirus epizootics has recently raised concerns on account of their considerable population-level impacts.[1,13] Despite this fact, the origin of ranaviruses and factors underlying their emergence remain generally undiscovered. For any given disease outbreak, much of the debate focuses on two hypotheses that answer questions about its origin. The novel pathogen hypothesis (NPH) assumes that the pathogen has recently spread into naive geographic areas. Although the endemic pathogen hypothesis (EPH) suggests that the pathogen has been already present in the environment and become more virulent owing to a change in the ecological, immunological, and/or behavioral parameters of the host or parasite.[14,15] Climate is one of the important environmental factors influencing the emergence of infectious diseases.[16] Laboratory experiments showed that Ranavirus proliferation, disease incidents, and mortality rate increase at higher temperatures. Moreover, the frequency of reports of ranavirosis reports in the UK has also been correlated with historic climate warming in the 1990s.[17] Yet, although ranaviruses are globally distributed, the disease outbreaks seem to be inconsistent and geographically unrelated.[8] This raises the question of whether ongoing climate warming may trigger Ranavirus emergence and be responsible for the still growing number of incidents.

[1]Asociación Herpetológica Española (AHE), Madrid, Spain

[2]Museo Nacional de Ciencias Naturales (MNCN-CSIC), Madrid, Spain

[3]Scottish Qualifications Authority, Glasgow, Scotland, UK

[4]Department of Zoology, Hungarian Natural History Museum, Budapest, Hungary

[5]Laboratory for Molecular Taxonomy, Hungarian Natural History Museum, Budapest, Hungary

[6]CRARC, Catalonian Reptiles and Amphibians Rescue Centre, Masquefa, Barcelona, Spain

[7]Institute of Zoology, Zoological Society of London, Regents Park, LondonNW1 4RY, UK

[8]Centre for Ecology, Evolution and Environmental Changes (cE3c), Faculdade de Ciências, Universidade de Lisboa, Lisboa, Portugal

[9]IMIB-Biodiversity Research Institute (University of Oviedo-CSIC-Principality of Asturias), Mieres, Spain

[10]Lead contact

*Correspondence: jaime.bosch@csic.es

https://doi.org/10.1016/j.isci.2022.105541

Please cite this article in press as: Thumsová et al., Climate warming triggers the emergence of native viruses in Iberian amphibians, iScience (2022), https://doi.org/10.1016/j.isci.2022.105541

We analyzed and sequenced samples from amphibian carcasses collected in 15 never-before-studied incidents that occurred in Iberia between 1988 and 2020. We then conducted genetic characterization of these viruses to (1) investigate their phylogenetic relationship with other previously sequenced ranaviruses from around the globe and to (2) study patterns of their diversity. Finally, we investigated whether climate warming could be triggering some of the ranavirosis outbreaks described here.

RESULTS AND DISCUSSION

Disease and mass mortality

We repeatedly encountered numerous dead or living amphibian individuals of different life stages with systemic hemorrhage, skin ulceration or extensive tissue necrosis in several geographically distant regions of Iberia. These overt signs of disease accompanied by host mass mortality are usually attributed to ranavirosis.[18,19] Here, we analyzed data representing 15 novel incidents that occurred between 1988 and 2020 inclusive (Table 1). Most incidents were located within Spanish territory, but also included two cases in the French Pyrenees (~1 km away from the Spanish border). Our study cases occurred across a broad range of altitudes, from 9 to 1996 m above sea level (asl). However, the majority of sites (10 of the 15) were located within mountain areas exceeding 1,000 m asl. In just two study sites, we did not observe mortalities or mass die-offs on any occasion, but live individuals at both of these sites were observed (and sampled) exhibiting clear signs of ranavirosis. It is expected that amphibian mortality incidents will often go unnoticed, especially as a consequence of sampling design and lack of regular population monitoring.[20,21] We used targeted qPCR testing to screen 42 individuals from six amphibian species for ranavirus infection: 18 individuals of Common midwife toad (*Alytes obstetricans*), ten Palmate newts (*Lissotriton helveticus*), eight Sharp-ribbed salamanders (*Pleurodeles waltl*), three Pyrenees frogs (*Rana pyrenaica*), two Moller's tree frogs (*Hyla molleri*) and one Western spadefoot (*Pelobates cultripes*). Six incidents (40%) involved disease in more than one species; five of these involved two species and the remaining one involved three species.

Molecular diagnostics confirmed Ranavirus infection in 34 of the 42 individuals of different life stages from the 15 studied incidents. Prevalence of infection reached 60.0% in *L. helveticus*, 77.8% in *A. obstetricans* and 100% in *P. waltl*, *R. pyrenaica*, *H. molleri* and *P. cultripes*. The estimated infection loads varied from 9.2 to more than 60 million genomic equivalents of virions, with the highest quantity found in dead specimen of *R. pyrenaica* from Ordesa y Monte Perdido National Park (PNOMP) (Table 1). Overall, infection loads of dead and diseased individuals of *R. pyrenaica* are the highest values ever recorded in Iberia.[1,22,23] Specimens of *A. obstetricans* from the first epizootic episode recorded in Spain, and misdiagnosed as red-leg syndrome,[6] also tested positive for ranavirus. This adds the incident to the list of the earliest known mortality incidents caused by ranaviruses in Europe, with similar timing of emergence as outbreaks in Croatia and the UK.[18,24]

Phylogeny of ranaviruses

We performed ranavirus genotyping of the samples presenting the highest ranavirus quantities from each of the 15 sites. We targeted the MCP gene, five partial sequences from CMTV open reading frames (ORFs) and an intergenic region.[1] We obtained a complete set of the targeted loci from three samples. We were able to amplify the MCP gene, the intergenic region, and three or four of the partial ORF loci from a further four samples. From one sample we only obtained a sequence from the MCP gene and, for the remaining samples, we retrieved sequences from all loci except for the MCP gene (Table 1). Sequences from amplification products of six loci using three isolates from this study were aligned against ranavirus whole genomes from the NCBI nucleotide database and concatenated to form an alignment of 2058 base pairs (bp) in length. We did the same with sequences from amplification products of five loci using four isolates from this study to form a concatenated alignment of 1,571 bp in length. Phylogenetic assessment of the concatenated sequences, derived from animals of four incidents, revealed four completely new genotypes. Three of these were grouped with CMTV-like viruses and the remaining one with FV3-like viruses (Figures 1 and S1).

To more effectively overlay the geographical locations of isolates onto the phylogeny, we generated an additional phylogenetic tree which compared alignment length against geographical range and coverage by including other viruses with partially sequenced genomes in the NCBI nucleotide database. We used five isolates from this study, our isolates from Picos de Europa National Park (PNPE) and Galicia,[1] isolates from Portugal[22,25] and others from around the world in addition to the viruses with whole genomes used

Please cite this article in press as: Thumsová et al., Climate warming triggers the emergence of native viruses in Iberian amphibians, iScience (2022), https://doi.org/10.1016/j.isci.2022.105541

Table 1. List of study incidents and analyzed samples

Locality and region	Geographic coordinates (latitude, longitude)	Altitude (masl)	First disease outbreak	Species mortality	Sampling year	Sample id	Sample species	Sample life history stage	Tissue sample	Sequenced genes	Infection load (GE)	Phylogenetic assessment
Ibón de Piedrafita, Huesca	42.70, −0.36	1,611	signs of disease (1988), mass mortality (1992)	Ao, Bs, fish	1988	HUEIDP_Ao_1988	Ao	hindlimbs larvae	liver + toe clip	none	9	none
					2011	HUEIDP_Ao_1992-1994	Ao	adult	toe clip	13R	14	none
Villavieja del Lozoya, Madrid	41.00, −3.69	1,077	mass mortality (2007)	Pw	2007	MADVDL_Pw_2007	Pw	adult	liver	16L, 13R, 22L, 58L, 59R	418	CMTV-like
Arlet, French Pyrenees	42.84, −0.61	1996	mortality (2008)	Rt	2017	PFRARG_Ao_NA	Ao	metamorph	liver	none	76	none
Puits d'Arious, French Pyrenees	42.86, −0.63	1884	signs of disease (2008)	–	2017	PFRPUI_Ao_NA	Ao	metamorph	liver	16L	57	look like FV3-like
Navajo de Peribáñez, Albacete	38.90, −2.44	1,024	mass mortality (2013)	Pw	2013	ALBNDP_Pw_2013	Pw	adult	liver	16L, 82L, 13R, 22L, 58L, 59R	2,263,210	CMTV-like
Gorrondatxe, Bizkaia	43.38, −3.01	9	mortality (2016)	Lh	2016	PVAGOR_Lh_2016	Lh	adult	liver + toe clip	22L	43	none
Puerto de Canencia, Madrid	40.93, −3.60	1,002	mortality (2016)	Pc	2020	MADPDC_Hm_2020	Hm	larvae	liver + toe clip	16L, 82L, 13R, 58L, 59R	182,080	CMTV-like
Coto Bello, Asturias	43.13, −5.64	1,241	mortality (2016)	Ao, Tm	2020	ASTCBE_Ao_2020	Ao	larvae	tail clip	16, 82, 22L, 59R	5,761,582	CMTV-like
Nocedo, Burgos	42.75, −3.72	1,017	mortality (2017)	Ao	2017	BURNOC_Ao_2017	Ao	OW larvae	liver	16L, 82L, 13R, 22L, 58L, 59R	4,712	FV3-like
Corrales del Vino, Zamora	41.28, −5.71	856	mass mortality (2017)	Pw, Pp	2018	ZAMCDV_Pw_2018	Pw	adult	liver	16L, 82L, 13R, 22L, 59R	3,747,052	CMTV-like
Barranco Fuen Berna, Huesca	42.62, −0.03	1749	mass mortality (2017)	Rp	2020	PNOBFB_Rp_2020	Rp	adult	liver + toe clip	16L, 82L, 13R, 22L, 58L, 59R	60,910,311	CMTV-like
Ibón de Acherito, Huesca	42.88, −0.71	1880	signs of disease (2018)	–	2018	ARAACH_Lh_2018	Lh	adult	tail clip	none	1,067	none
Zamalvide, Gipuzkoa	43.30, −1.92	197	mortality (2018)	Lh	2018	PVAZAM_Lh_2018	Lh	adult	liver + skin	none	24	none
Parque El barranco, Zaragoza	41.62, −0.89	257	mortality (2018)	Ao	2018	ZARPEB_Ao_2018	Ao	metamorph	liver + toe clip	none	14	none
Urkabustaiz, Alava	42.99, −2.96	583	mortality (2020)	Lh	2020	ALACBU_Lh_2020	Lh	adult	liver + skin	82L, 13R, 22L, 58L, 59R	109	look like CMTV-like

Abbreviations key: Ao, *Alytes obstetricans*; Bs, *Bufo spinosus*; Hm, *Hyla molleri*; Lh, *Lissotriton helveticus*; Pc, *Pelobates cultripes*; Pp, *Pelophylax perezi*; Pw, *Pleurodeles waltl*; Rp, *Rana pyrenaica*; Rt, *Rana temporaria*; Tm, *Triturus marmoratus*; GE, genomic equivalent of virions.

CellPress
OPEN ACCESS

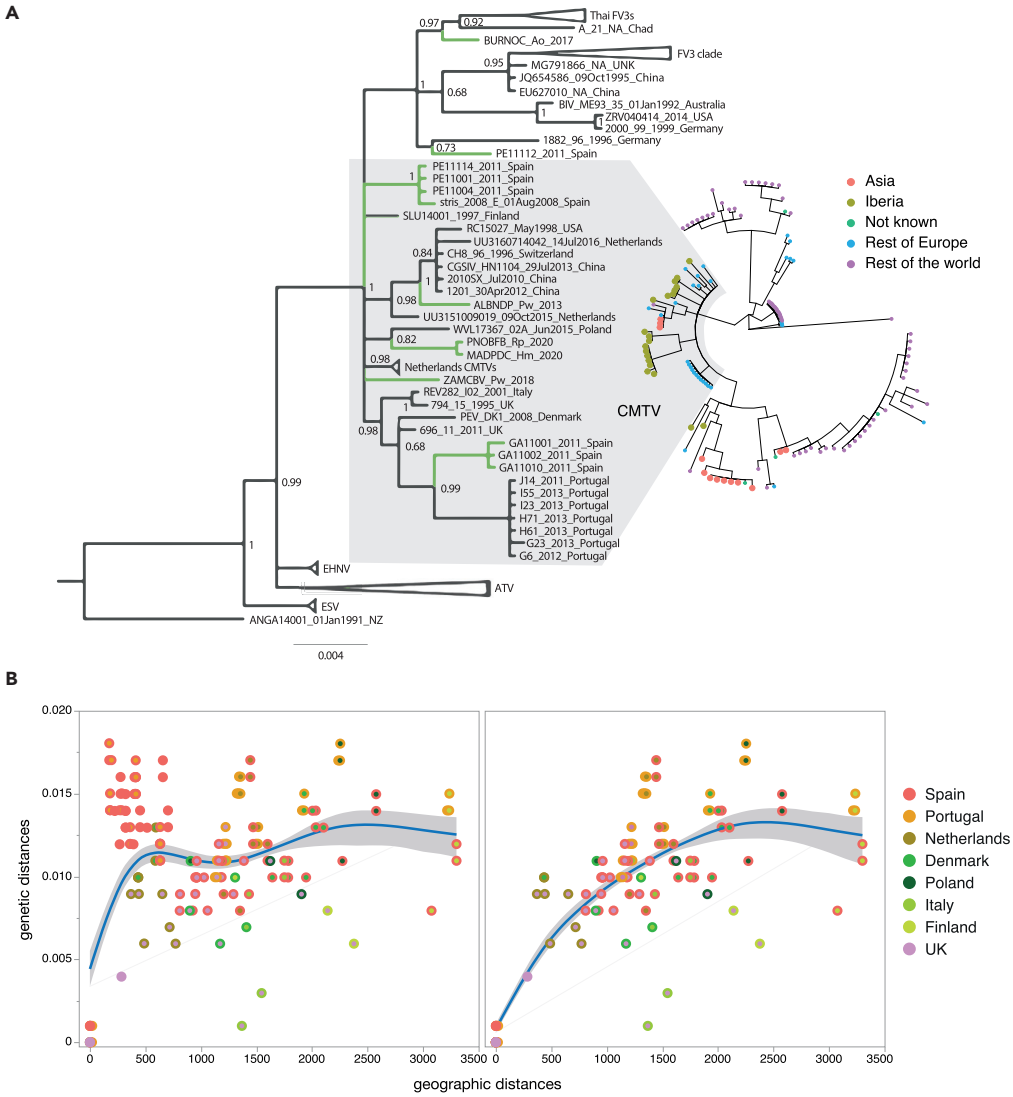

Figure 1. Phylogenetic relationships of ranaviruses and genetic diversity among CMTVs

(A) Phylogenetic relationships among ranaviruses visualised as a simple dendrogram with labeled tips and branches leading to Spanish isolates marked in green (left) and an alternative visualization highlighting geographic origin (country of isolation; right). The CMTV group is shaded gray. The color and size of points indicate geographic region; large points are used to emphasize isolates from Iberia and Asia and small points are used for remaining regions. Regions are defined according to their relevance to attempts to untangle the emergence of CMTV: Iberia is distinguished from the rest of Europe and Asia as the three regions where almost all incidents of CMTV infection have been observed and the remainder of Ranavirus included are either of unknown origin or labeled the rest of the world. The phylogeny was generated from a concatenated alignment (1,571 bp in length) containing many viruses lacking sequence data for some of the loci and was trimmed manually, attempting to balance alignment length and the number and geographical coverage of the retained isolates. The tree was constructed with Mr. Bayes using the GTR model of molecular evolution and 1 million generations. Node support values are posterior probabilities expressed as decimals. Full names and accession numbers for all isolates are given in Table S7.

(B) Evidence of isolation by distance in CMTVs and two independent dispersal routes of CMTV through the Iberian Peninsula. Plots show pairwise genetic distances among CMTVs calculated from the same alignment which generated the phylogeny in (A). The correlation between geographic and genetic distances in CMTVs (left) is partially masked by the inclusion of pairs comprising a CMTV from the west of Iberia and one from the center or east of the peninsula (right).

previously and found considerable ranavirus diversity in Iberia (Figure 1A, Table S7). A novel isolate from Nocedo (BURNOC_Ao_2017), which caused a disease outbreak in *A. obstetricans* larvae, is an FV3-like virus but is distinct from the isolate from the Ándara lake (PE11112_2011) sequenced by Price et al.[1]

Please cite this article in press as: Thumsová et al., Climate warming triggers the emergence of native viruses in Iberian amphibians, iScience (2022), https://doi.org/10.1016/j.isci.2022.105541

Relationships within CMTV are poorly resolved, likely due to the limited resolution of the targeted genes. Despite a final concatenated alignment with 1,571 bp in length, CMTV-like viruses do not form a monophyletic group here in contrast to phylogenies generated from alignments which use whole genome data.[26] Yet, difficulties resolving relationships within the clade are also shared by studies where whole genomes are available. Despite this, it is clear that a large number of distinct CMTVs are found in Iberia (Figures 1A and S1). The virus which we isolated from *P. waltl* found in Navajo de Peribáñez in Albacete (ALBNDP_Pw_2013) formed a well-supported cluster with recombinant *Rana catesbiana* virus I (RCV-Z) from the USA, a virus from the Netherlands, *Testudo hermanni* ranavirus (THRV) isolated in Switzerland from a captive tortoise, and Chinese giant salamander viruses (*Andrias davidianus* ranavirus [ADRV] and Chinese giant salamander iridovirus [CGSIV]) from China. Identical isolates from *R. pyrenaica* found in the PNOMP in Huesca (PNOBFB_Rp_2020) and from *H. molleri* found in Puerto de Canencia in Madrid (MADPDC_Hm_2020) grouped with a virus from a non-native red-eared slider from Poland (WVL17367_02A_Jun2015; posterior probability Pp = 0.82). Bosca's newt virus (BNV[1]) and Portuguese newt and toad ranavirus (PNTRV[22]) isolated from amphibians in the northwest of Iberia (Spain and Portugal respectively) formed a distinct, well-supported clade (Pp = 0.99).

The major capsid protein gene phylogeny of ranaviruses from around the world then grouped other two Spanish isolates (from Coto Bello and Villavieja del Lozoya) with CMTV-like viruses and also highlighted a great diversity in Spain (Figure S2). Even though the MCP gene is a short DNA sequence with low diversity generating trees with less sequence information than using a complete suite of Ranavirus loci, it has been routinely used to genotype ranaviruses and is the most sequenced locus in the genome.[27] The MCP tree, therefore, provides an opportunity to visualize the diversity of Iberian ranaviruses in the context of practically all sampled Ranavirus diversity. Isolate JN590256 from *A. davidianus* sampled in a salamander farm in China (Figures 1A and S2) has five completely unique single nucleotide polymorphisms (SNPs) not present in any other viruses in the alignment. These differences cause the very long branch seen in Figure S2 and seem likely to be errors and for this reason the isolate was removed from subsequent analyses.

Time-calibrated phylogeny with phylogeographical inference revealed phylogenetic tree with poorly supported clades for CMTVs. Bayesian phylogeography indicated more basal CMTV-like lineages being in Iberia and, specifically, Western Iberia seems represent the most probable origin of the lineage (Figure S3). Based on tip-dates and the substitution rate, the root for the entire CMTV-like lineage was estimated around 840 years before present (95% high posterior density, 464 to 1,297). This estimate is relatively consistent with the estimate for CMTV-like lineage published by Vilaça et al.[28] Our results indicated that CMTV-like lineage has been present in Iberia for centuries. CMTVs found in the UK and the Netherlands likely coming from Iberia originated between 337 and 890 years ago, and between 265 and 770 years ago respectively. CMTVs in China that were isolated from captive individuals have a more recent origin, likely mutated from the Netherlands' CMTVs around 123 years ago (95% high posterior density, 48 to 215). However, given the low within-clade resolution phylogenetic relationships and time calibration must be taken with caution. We do not consider the age of key nodes as absolute dates but only relative estimates to distinguish that some CMTVs can be more ancient than others.

Genetic diversity in CMTV

To study patterns of CMTV diversity further we removed viruses from the FV3 and ATV clades (and other related fish viruses). Mean and maximum pairwise genetic distances were calculated within countries where viruses were isolated, first from the alignment of partial MCP gene sequences (Table S1) and then from the alignment of concatenated partial gene sequences where alignment length and geographical coverage were balanced (Table S2). These analyses confirmed the considerable diversity in Iberian CMTVs observed in the phylogenies: Iberian CMTVs showed greater diversity than CMTVs from the rest of the world combined. Maximum pairwise genetic distances for Iberian CMTVs compared to the rest of Europe (calculated from MCP gene sequences), were higher for Iberia (0.0179 versus 0.0134 respectively). In addition, five parameters including the number of polymorphic sites (S), the average number of differences (k), nucleotide diversity (π), Theta (θ)-W per sequence and Theta (θ)-W per site were used to measure the DNA polymorphism of DNA sequences within countries where viruses were isolated. The highest DNA polymorphism was confirmed for Iberian CMTVs, especially for the Spanish ones (Table S3). Nucleotide diversity, Theta-W per sequence and per site for Iberian isolates was 0.0115, 12.3578, 0.0122, respectively. The out of Iberian CMTVs retained only 53.3% of 0.0061 nucleotide diversity, 62.9% of 7.7734 Theta-W per sequence and 62.9% of 0.0077 Theta-W per site found in Iberia. Analysis in pairwise comparisons also

confirmed greater diversity for Iberian CMTVs. Our data indicated 76 versus 95 pairwise comparisons in Iberian versus out of Iberian CMTVs, respectively. Out of Iberian CMTVs retained only around 53% of 0.0061 nucleotide diversity found in Iberia (Table S3).

The spread of an amphibian pathogen by natural (local) dispersal of hosts is expected to yield a correlation between genetic and geographic distance in which the pathogen exhibits isolation by distance.[29] However, we found no relationship between pairwise genetic and geographic distances in Iberian CMTVs at the resolution offered by these genetic data, suggesting that there is no signature of spread by natural dispersal. The fitted line of pairwise genetic distances versus geographic distances is effectively flat (Figure S4). However, there is a relationship of increasing genetic distance with geographical distance when we look at CMTVs as a whole (Figure 1B). Initially, this relationship is partly masked by a subset of pairwise comparisons generated from nearby but highly divergent viruses (Figure 1B top) but when these comparisons are excluded a strong linear relationship is apparent (Figure 1B bottom). The comparisons that were excluded almost entirely comprise comparisons between Iberian CMTVs: 77 of them involve a Spanish virus and a Portuguese virus, 24 of them involve two Spanish viruses (always a Galician [north-west Spain] BNV virus and a virus from eastern Spain [Table S5]) and just 2 involve viruses from elsewhere (Table S4).

The main linear relationship of increasing genetic distance with geographical distance suggests that CMTV has spread across Europe by natural dispersal (China is a separate case likely involving introduction from Europe which is also supported by our supergene phylogeny and time-calibrated phylogeography, Figures 1A and S3). The pairs which do not sit on this line, where one member of each pair comprises a virus from western Iberia (the monophyletic group formed by Galician BNV and Portuguese PNTRV [Figure 1A]) and a virus from elsewhere in Iberia, suggests two separate dispersal routes for CMTV in Iberia, one in the west and another in the central/eastern region.

The exact origin and drivers for the emergence of CMTV remain uncertain. However, our results indicate that CMTV-like lineage has been present in Iberia for centuries, presenting considerable genetic diversity compared to the isolates from the rest of the world with no pattern of regional spread, supporting endemicity in this area. Accordingly, we suggest that CMTV could be a European clade with the Iberian Peninsula as its diversity hotspot and thus, probably containing the CMTVs' ancestral population. An East-West division of Iberian CMTV viruses may suggest that the viruses have been dispersing from genetically distinct source populations independently on each side of the Iberian region. From the data available here, we cannot say exactly, but one hypothesis explaining the pattern found in this study is that CMTVs have spread together with their hosts out of Spain to the rest of Europe, out of which they were introduced to other parts of the world. This hypothesis is also supported by the wide diversity among CMTVs in Europe, which is generally consistent with spread by natural dispersal, and by the fact that phylogenetic analysis shows European CMTVs at the root of the clade whereas the non-European CMTVs at the tip of the clade. It is also possible (given the low confidence in branching patterns within CMTV clade in phylogenies), of course, that CMTV emerged outside of the Iberian Peninsula and traveled over the Pyrenees in the opposite direction. More sampling accompanied by phylogenetic studies focusing especially on geographical areas outside Europe is crucial to fully evaluate the evolutionary history of CMTV ranaviruses.

Effect of temperature on the CMTVs driven mortality events

The patterns of evolutionary history found here together with the evidence that CMTVs in Iberia are widely distributed, with disease outbreaks being extremely patchy[13,23] and highly seasonal (more frequent and more severe at higher temperatures[17]), offer support to the EPH. With the exception of one event (Zamora site), all CMTV-driven outbreaks studied here occurred in the sites exceeding 1,000 m. The high degree of genetic isolation and extreme climate conditions make mountain populations highly susceptible to infections.[30] Climate change, which is more acute particularly in mountain areas, can moreover force the severity of the infection and trigger an outbreak of the disease.[31,32] In all six mortality events unequivocally attributed to CMTV-like viruses, we checked whether there was a shift in the temperature regimen preceding the Ranavirus outbreaks. In all cases, we found a significant shift in the increasing rate of temperatures (in the case of Villavieja del Lozoya in Madrid and Navajo de Peribáñez in Albacete), or a significant increase in temperatures *per se* (in the remaining four cases, Table S6), at the exact time when the first mortalities were recorded at each place (Figure 2). This pattern

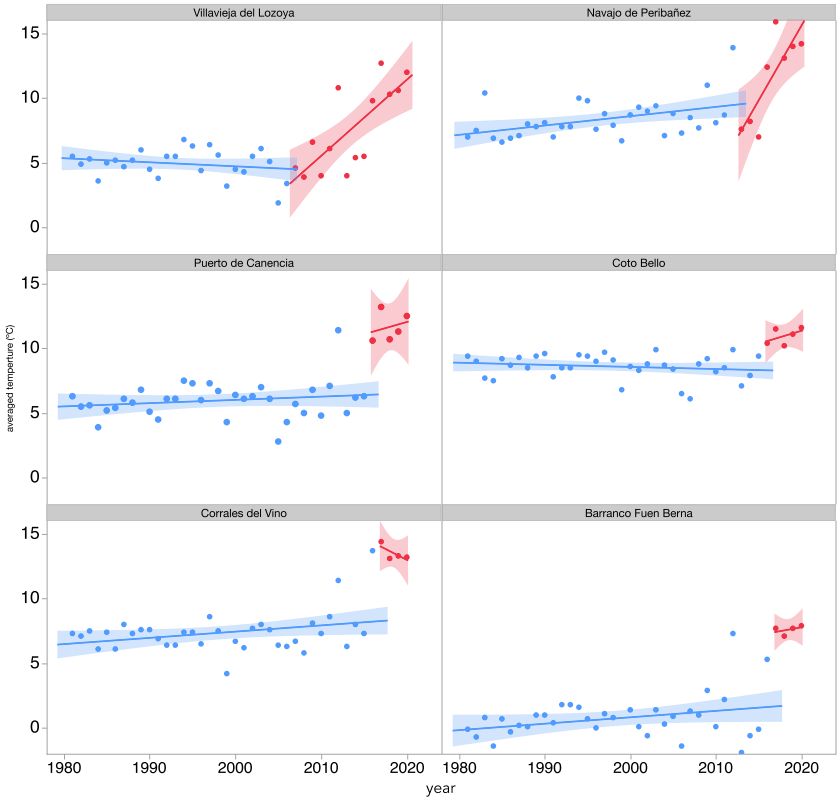

Figure 2. The onset of outbreaks of ranavirosis consistently coincides with climate warming at independent sites across Spain

Regression analyses between years and yearly averaged estimated temperatures before the first recorded mortality incident (cyan) and after that (red) at the exact six study localities where disease outbreaks were unequivocally attributed to CMTV-like ranaviruses.

has also been suggested by eDNA studies showing an increased prevalence of Ranavirus in the water during summer months, coinciding with higher water temperatures.[33,34] Given the pristine nature of almost all study localities, we consider it unlikely that other ecological perturbances, such as pollution, could have contributed to the observed disease outbreaks.

In conclusion, we found CMTV-like viruses could be a European clade with the Iberian Peninsula looking as the probable center of diversity. Diversity among CMTVs in Europe is consistent with spread by natural dispersal. Our phylogenetic analyses show the presence of independent CMTV lineages in the Iberian Peninsula that could have spread into the rest of Europe and subsequently be introduced to the rest of the world. The endemic status of CMTVs in Iberia is supported by evidence that climate warming is triggering the emergence of ranavirosis. However, given the fact that new isolates may be still discovered, we consider it premature from the data available here to infer the origin of CMTV-like ranaviruses and we call that more studies are urgently needed.

Limitations of the study

Despite our efforts to sequence *Ranavirus* isolates from all carcasses collected, some partial ORF loci remained unsequenced (Table 1) possibly owing to the state of degradation of the tissues. Furthermore, some relationships within the CMTV clade are still poorly resolved; however, difficulties to resolve these relationships are shared also by studies where whole genomes are available.[26] As typical of studies undertaking molecular phylogenetics, the addition of new isolates is likely to refine our hypothesis. Even though our findings are accompanied by uncertainties, these results shed new light on the possible origin and drivers for the emergence of CMTV ranaviruses, which have long been uncertain.

STAR★METHODS

Detailed methods are provided in the online version of this paper and include the following:

- KEY RESOURCES TABLE
- RESOURCE AVAILABILITY
  - Lead contact
  - Materials availability
  - Data and code availability
- EXPERIMENTAL MODEL AND SUBJECT DETAILS
  - Sampling
- METHOD DETAILS
  - DNA extraction and ranavirus detection
  - Sequencing and phylogenetics
- QUANTIFICATION AND STATISTICAL ANALYSIS

SUPPLEMENTAL INFORMATION

Supplemental information can be found online at https://doi.org/10.1016/j.isci.2022.105541.

ACKNOWLEDGMENTS

We thank R. Márquez, G. Alarcos, C. Tejado, A. Sánchez, A. Portal, the people working at PNOMP (especially F. Villaespesa, F. Carmona, I. Gómez), rangers of Agentes Forestales of Comunidad de Madrid and members of the Aranzadi science society for sampling supply, and the personal of the Molecular Systematics Laboratory of Museo Nacional de Ciencias Naturales of Madrid (L. Alcaraz, I. Acevedo, R. García and M. Gutiérrez-Ray) for laboratory support. David Lesbarrères and an anonymous reviewer provided useful comments that helped improve the manuscript. BT was supported by 'Doctorados Industriales de la Comunidad de Madrid' (Ref. IND2020/AMB-17438). This work was supported by Organismo Autónomo Parques Nacionales of Spain (ref. 2399/2017; PI: JB), Foundation for the Conservation of Salamanders (project "Monitoring the incidence of emerging pathogens on endemic urodeles from the Cantabrian range, Spain"; PI: BT), and Fundação para a Ciência e a Tecnologia (Ref. PTDC/BIA-CBI/2434/2021; PI: GMR, Co-PI: JB).

AUTHOR CONTRIBUTIONS

J.B., B.T., and S.J.P. conceived the ideas and designed the methodology. J.B. and B.T. collected the samples, acquired funding and performed statistical analyses. V.G.C. performed spatial analyses. B.T. performed molecular screening and processed samples for sequencing. J.V. aligned sequences. S.J.P. carried out phylogenetic analyses. A.M. and G.M.R. advised on phylogenetic analyses and interpretation. B.T. and S.J.P. prepared the manuscript, which was revised by all authors.

DECLARATION OF INTERESTS

The authors declare no competing interests.

Received: April 25, 2022
Revised: September 19, 2022
Accepted: November 7, 2022
Published: November 29, 2022

REFERENCES

1. Price, S.J., Garner, T.W.J., Nichols, R.A., Balloux, F., Ayres, C., Mora-Cabello de Alba, A., and Bosch, J. (2014). Collapse of amphibian communities due to an introduced ranavirus. Curr. Biol. *24*, 2586–2591. https://doi.org/10.1016/j.cub.2014.09.028.

2. Scheele, B.C., Pasmans, F., Skerratt, L.F., Berger, L., Martel, A., Beukema, W., Acevedo, A.A., Burrowes, P.A., Carvalho, T., Catenazzi, A., et al. (2019). Amphibian fungal panzootic causes catastrophic and ongoing loss of biodiversity. Science *363*, 1459–1463. https://doi.org/10.1126/science.aav0379.

3. Bosch, J., Martínez-Solano, I., and García-París, M. (2001). Evidence of a chytrid fungus infection involved in the decline of the common midwife toad (Alytes obstetricans) in protected areas of Central Spain. Biol. Conserv. *97*, 331–337.

4. Walker, S.F., Bosch, J., Gomez, V., Garner, T.W.J., Cunningham, A.A., Schmeller, D.S., Ninyerola, M., Henk, D.A., Ginestet, C., Arthur, C.-P., and Fisher, M.C. (2010). Factors driving pathogenicity vs. prevalence of amphibian panzootic chytridiomycosis in Iberia. Ecol. Lett. *13*, 372–382. https://doi.org/10.1111/j.1461-0248.2009.01434.x.

5. Rosa, G.M., Anza, I., Moreira, P.L., Conde, J., Martins, F., Fisher, M.C., and Bosch, J. (2013).

Evidence of chytrid-mediated population declines in common midwife toad in Serra da Estrela, Portugal. Anim. Conserv. *16*, 306–315. https://doi.org/10.1111/j.1469-1795.2012.00602.x.

6. Márquez, R., Olmo, J.L., and Bosch, J. (1995). Recurrent mass mortality of larval midwife toads Alytes obstetricans in a lake in the Pyrenean mountains. Herp. J. *5*, 287–289.

7. Schock, D.M., Bollinger, T.K., Gregory Chinchar, V., Jancovich, J.K., and Collins, J.P. (2008). Experimental evidence that amphibian ranaviruses are multi-host pathogens. Copeia *2008*, 133–143. https://doi.org/10.1643/CP-06-134.

8. Duffus, A.L.J., Waltzek, T.B., Stöhr, A.C., Allender, M.C., Gotesman, M., Whittington, R.J., Hick, P., Hines, M.K., and Marschang, R.E. (2015). Distribution and host range of ranaviruses. In Ranaviruses: Lethal Pathogens of Ectothermic Vertebrates, M.J. Gray and V.G. Chinchar, eds. (Springer International Publishing), pp. 9–57. https://doi.org/10.1007/978-3-319-13755-1_2.

9. Granoff, A., Came, P.E., and Rafferty, K.A. (1965). The isolation and properties of viruses from Rana pipiens: their possible relationship to the renal adenocarcinoma of the leopard frog. Ann. N. Y. Acad. Sci. *126*, 237–255. https://doi.org/10.1111/j.1749-6632.1965.tb14278.x.

10. Jancovich, J.K., Steckler, N.K., and Waltzek, T.B. (2015). Ranavirus taxonomy and phylogeny. In Ranaviruses: Lethal Pathogens of Ectothermic Vertebrates, M.J. Gray and V.G. Chinchar, eds. (Springer International Publishing), pp. 59–70. https://doi.org/10.1007/978-3-319-13755-1_3.

11. Claytor, S.C., Subramaniam, K., Landrau-Giovannetti, N., Chinchar, V.G., Gray, M.J., Miller, D.L., Mavian, C., Salemi, M., Wisely, S., and Waltzek, T.B. (2017). Ranavirus phylogenomics: signatures of recombination and inversions among bullfrog ranaculture isolates. Virology *511*, 330–343. https://doi.org/10.1016/j.virol.2017.07.028.

12. Deng, L., Geng, Y., Zhao, R., Gray, M.J., Wang, K., Ouyang, P., Chen, D., Huang, X., Chen, Z., Huang, C., et al. (2020). CMTV-like ranavirus infection associated with high mortality in captive catfish-like loach, Triplophysa siluorides in China. Transbound. Emerg. Dis. *67*, 1330–1335. https://doi.org/10.1111/tbed.13473.

13. Bosch, J., Mora-Cabello de Alba, A., Marquínez, S., Price, S.J., Thumsová, B., and Bielby, J. (2021). Long-Term monitoring of amphibian populations of a National Park in Northern Spain reveals negative persisting effects of Ranavirus, but not Batrachochytrium dendrobatidis. Front. Vet. Sci. *8*, 645491. https://doi.org/10.3389/fvets.2021.645491.

14. Carey, C. (1993). Hypothesis concerning the causes of the disappearance of boreal toads from the mountains of Colorado. Conserv. Biol. *7*, 355–362.

15. Rachowicz, L.J., Hero, J.-M., Alford, R.A., Taylor, J.W., Morgan, J.A., Vredenburg, V.T., Collins, J.P., and Briggs, C.J. (2005). The novel and endemic pathogen hypotheses: competing explanations for the origin of emerging infectious diseases of wildlife. Conserv. Biol. *19*, 1441–1448. https://doi.org/10.1111/j.1523-1739.2005.00255.x.

16. Epstein, P.R. (2001). Climate change and emerging infectious diseases. Microbes Infect. *3*, 747–754. https://doi.org/10.1016/s1286-4579(01)01429-0.

17. Price, S.J., Leung, W.T.M., Owen, C.J., Puschendorf, R., Sergeant, C., Cunningham, A.A., Balloux, F., Garner, T.W.J., and Nichols, R.A. (2019). Effects of historic and projected climate change on the range and impacts of an emerging wildlife disease. Glob. Chang. Biol. *25*, 2648–2660. https://doi.org/10.1111/gcb.14651.

18. Cunningham, A.A., Langton, T.E., Bennett, P.M., Lewin, J.F., Drury, S.E., Gough, R.E., and Macgregor, S.K. (1996). Pathological and microbiological findings from incidents of unusual mortality of the common frog (Rana temporaria). Philos. Trans. R. Soc. Lond. B Biol. Sci. *351*, 1539–1557. https://doi.org/10.1098/rstb.1996.0140.

19. Gray, M.J., Miller, D.L., and Hoverman, J.T. (2009). Ecology and pathology of amphibian ranaviruses. Dis. Aquat. Organ. *87*, 243–266. https://doi.org/10.3354/dao02138.

20. Price, S.J., Wadia, A., Wright, O.N., Leung, W.T.M., Cunningham, A.A., and Lawson, B. (2017). Screening of a long-term sample set reveals two Ranavirus lineages in British herpetofauna. PLoS One *12*, e0184768. https://doi.org/10.1371/journal.pone.0184768.

21. Hall, E.M., Crespi, E.J., Goldberg, C.S., and Brunner, J.L. (2016). Evaluating environmental DNA-based quantification of ranavirus infection in wood frog populations. Mol. Ecol. Resour. *16*, 423–433. https://doi.org/10.1111/1755-0998.12461.

22. Rosa, G.M., Sabino-Pinto, J., Laurentino, T.G., Martel, A., Pasmans, F., Rebelo, R., Griffiths, R.A., Stöhr, A.C., Marschang, R.E., Price, S.J., et al. (2017). Impact of asynchronous emergence of two lethal pathogens on amphibian assemblages. Sci. Rep. *7*, 43260. https://doi.org/10.1038/srep43260.

23. von Essen, M., Leung, W.T.M., Bosch, J., Pooley, S., Ayres, C., and Price, S.J. (2020). High pathogen prevalence in an amphibian and reptile assemblage at a site with risk factors for dispersal in Galicia, Spain. PLoS One *15*, e0236803. https://doi.org/10.1371/journal.pone.0236803.

24. Fijan, N., Matašin, Z., Petrinec, Z., Valpotić, I., and Zwillenberg, L.O. (1991). Isolation of an iridovirus-like agent from the green frog (Rana esculenta L.). Vet. Arh. Zagreb *61*, 151–158.

25. de Matos, A.P.A., Caeiro, M.F., Papp, T., Matos, B.A., Correia, A.C.L., and Marschang, R.E. (2011). New viruses from Lacerta monticola (Serra da Estrela, Portugal): further evidence for a new group of nucleo-cytoplasmic large deoxyriboviruses (NCLDVs). Microsc. Microanal. *17*, 101–108. https://doi.org/10.1017/S143192761009433X.

26. Price, S.J. (2015). Comparative genomics of amphibian-like ranaviruses, nucleocytoplasmic large DNA viruses of poikilotherms. Evol. Bioinform. Online *11*, 71–82. https://doi.org/10.4137/EBo.s33490.

27. Black, Y., Meredith, A., and Price, S.J. (2017). Detection and reporting of ranavirus in amphibians: evaluation of the roles of the world organisation for animal health and the published literature. J. Wildl. Dis. *53*, 509–520. https://doi.org/10.7589/2016-08-176.

28. Vilaça, S.T., Bienentreu, J.F., Brunetti, C.R., Lesbarrères, D., Murray, D.L., and Kyle, C.J. (2019). Frog virus 3 genomes reveal prevalent recombination between ranavirus lineages and their origins in Canada. J. Virol. *93*. 007655-19. https://doi.org/10.1128/JVI.00765-19.

29. Pybus, O.G., Tatem, A.J., and Lemey, P. (2015). Virus evolution and transmission in an ever more connected world. Proc. Biol. Sci. *282*, 20142878. https://doi.org/10.1098/rspb.2014.2878.

30. Haver, M., Le Roux, G., Friesen, J., Loyau, A., Vredenburg, V.T., and Schmeller, D.S. (2022). The role of abiotic variables in an emerging global amphibian fungal disease in mountains. Sci. Total Environ. *815*, 152735. https://doi.org/10.1016/j.scitotenv.2021.152735.

31. Bosch, J., Carrascal, L.M., Durán, L., Walker, S., and Fisher, M.C. (2007). Climate change and outbreaks of amphibian chytridiomycosis in a montane area of Central Spain; is there a link? Proc. Biol. Sci. *274*, 253–260. https://doi.org/10.1098/rspb.2006.3713.

32. Clare, F.C., Halder, J.B., Daniel, O., Bielby, J., Semenov, M.A., Jombart, T., Loyau, A., Schmeller, D.S., Cunningham, A.A., Rowcliffe, M., et al. (2016). Climate forcing of an emerging pathogenic fungus across a montane multihost community. Philos. Trans. R. Soc. Lond. B Biol. Sci. *371*, 20150454. https://doi.org/10.1098/rstb.2015.0454.

33. Miaud, C., Arnal, V., Poulain, M., Valentini, A., and Dejean, T. (2019). eDNA increases the detectability of ranavirus infection in an alpine amphibian population. Viruses *11*, 526.

34. Vilaça, S.T., Grant, S.A., Beaty, L., Brunetti, C.R., Congram, M., Murray, D.L., Wilson, C.C., and Kyle, C.J. (2020). Detection of spatiotemporal variation in ranavirus distribution using eDNA. Environ. DNA *2*, 210–220. https://doi.org/10.1002/edn3.59.

35. Leung, W.T.M., Thomas-Walters, L., Garner, T.W.J., Balloux, F., Durrant, C., and Price, S.J. (2017). A quantitative-PCR based method to estimate ranavirus viral load following normalisation by reference to an ultraconserved vertebrate target. J. Virol. Methods *249*, 147–155. https://doi.org/10.1016/j.jviromet.2017.08.016.

36. Mao, J., Hedrick, R.P., and Chinchar, V.G. (1997). Molecular characterization, sequence

analysis, and taxonomic position of newly isolated fish iridoviruses. Virology *229*, 212–220. https://doi.org/10.1006/viro.1996.8435.

37. Hall, T.A. (1999). BioEdit: a user-friendly biological sequence alignment editor and analysis program for Windows 95/98/NT. Nucl. Acids. Symp. Ser. *41*, 95–98. https://doi.org/10.14601/Phytopathol_Mediterr-14998u1.29.

38. Katoh, K., Misawa, K., Kuma, K.I., and Miyata, T. (2002). MAFFT: a novel method for rapid multiple sequence alignment based on fast Fourier transform. Nucleic Acids Res. *30*, 3059–3066. https://doi.org/10.1093/nar/gkf436.

39. Waterhouse, A.M., Procter, J.B., Martin, D.M.A., Clamp, M., and Barton, G.J. (2009). Jalview Version 2--a multiple sequence alignment editor and analysis workbench. Bioinformatics *25*, 1189–1191. https://doi.org/10.1093/bioinformatics/btp033.

40. R Core Team (2021). R: A Language and Environment for Statistical Computing (R Foundation for Statistical Computing). https://www.R-project.org/.

41. Paradis, E., Claude, J., and Strimmer, K. (2004). APE: analyses of phylogenetics and evolution in R language. Bioinformatics *20*, 289–290. https://doi.org/10.1093/bioinformatics/btg412.

42. Yu, G., Smith, D.K., Zhu, H., Guan, Y., and Lam, T.T. (2017). ggtree: an r package for visualization and annotation of phylogenetic trees with their covariates and other associated data. Methods Ecol. Evol. *8*, 28–36. https://doi.org/10.1111/2041-210X.12628.

43. Rozas, J., Ferrer-Mata, A., Sánchez-DelBarrio, J.C., Guirao-Rico, S., Librado, P., Ramos-Onsins, S.E., and Sánchez-Gracia, A. (2017). DnaSP 6: DNA sequence polymorphism analysis of large datasets. Mol. Biol. Evol. *34*, 3299–3302. https://doi.org/10.1093/molbev/msx248.

44. Suchard, M.A., Lemey, P., Baele, G., Ayres, D.L., Drummond, A.J., and Rambaut, A. (2018). Bayesian phylogenetic and phylodynamic data integration using BEAST 1.10. Virus Evol. *4*, vey016. https://doi.org/10.1093/ve/vey016.

45. Darriba, D., Taboada, G.L., Doallo, R., and Posada, D. (2012). jModelTest 2: more models, new heuristics and parallel computing. Nat. Methods *9*, 772. https://doi.org/10.1038/nmeth.2109.

46. Rambaut, A., Drummond, A.J., Xie, D., Baele, G., and Suchard, M.A. (2018). Posterior summarisation in Bayesian phylogenetics using Tracer 1.7. Syst. Biol. *67*, 901–904. https://doi.org/10.1093/sysbio/syy032.

47. Rambaut, A. (2019). Figtree v1.4.4. http://tree.bio.ed.ac.uk/software/figtree/.

48. Korbie, D.J., and Mattick, J.S. (2008). Touchdown PCR for increased specificity and sensitivity in PCR amplification. Nat. Protoc. *3*, 1452–1456. https://doi.org/10.1038/nprot.2008.133.

49. Huelsenbeck, J.P., and Ronquist, F. (2001). MRBAYES: Bayesian inference of phylogenetic trees. Bioinformatics *17*, 754–755. https://doi.org/10.1093/bioinformatics/17.8.754.

50. Altschul, S.F., Gish, W., Miller, W., Myers, E.W., and Lipman, D.J. (1990). Basic local alignment search tool. J. Mol. Biol. *215*, 403–410. https://doi.org/10.1016/S0022-2836(05)80360-2.

51. Guindon, S., and Gascuel, O. (2003). A simple, fast and accurate method to estimate large phylogenies by maximum-likelihood. Syst. Biol. *52*, 696–704. https://doi.org/10.1080/10635150390235520.

52. Fries, A., Rollenbeck, R., Nauß, T., Peters, T., and Bendix, J. (2012). Near surface air humidity in a megadiverse Andean mountain ecosystem of southern Ecuador and its regionalization. Agric. For. Meteorol. *152*, 17–30. https://doi.org/10.1016/j.agrformet.2011.08.004.

53. NASA/METI/AIST/Japan Spacesystems and U.S./Japan ASTER Science Team (2019). *ASTER Global Digital Elevation Model V003* [Data set] (NASA EOSDIS Land Processes DAAC). https://doi.org/10.5067/ASTER/ASTGTM.003.

STAR★METHODS

KEY RESOURCES TABLE

REAGENT or RESOURCE	SOURCE	IDENTIFIER
Biological samples		
Liver tissue and toe clips, see Table 1	dead amphibian specimens	N/A
Critical commercial assays		
DNAeasy Blood and Tissue kit	Qiagen GmbH, Hilden, Germany	Cat#69506
Probe 5′ VIC reporter, 3′ MGB-NFQ quencher TTATAGTAGCCTRTGCGCTTGGCC	Leung et al.[35]	N/A
SensiFAST™ Probe No-ROX Kit	Meridian Bioscience Inc.	Cat#BIO-86020
GoTaq® Green Master Mix	Promega Biotech Inc.	Cat#M7123
SYBR™ Safe DNA Gel Stain	Thermofisher Inc.	Cat#S33102
Deposited data		
Sequence data (deposited in GenBank, see Table S8)	This study	GenBank: OP_696786 – OP_696830
Oligonucleotides		
Primer: Major capsid protein gene (69), from CMTV ORF 16L, Forward: GTCTCTGGAGAA GAAGAA Reverse: GACTTGGCCACTTATGAC	Mao et al.[36]	N/A
Primer: Hypothetical protein gene, from CMTV ORF 13R, Forward: CTTCCCGTGTCTGGGTTGA Reverse: TGCACTCCGTAGCTCCTAAG	Price et al.[1]	N/A
Primer: Proliferating cell nuclear antigen gene, from CMTV ORF 22L, Forward: CAGTCCGTGTCTGTCG TAGA Reverse: CTCCGAAAACACCCAGGTTC	Price et al.[1]	N/A
Primer: p31k gene, from CMTV ORF 82L, Forward: ATCCTCTTTTCTTTCGGCGC Reverse: CCCTGCA CTTTTCCTTGACC	Price et al.[1]	N/A
Primer: Hypothetical protein gene, from CMTV ORF 58L, Forward: CCATGTACCCTCAGACCCTG Reverse: CATAGTCCGAACCCAAAGCG	Price et al.[1]	N/A
Primer: Hypothetical protein gene, from CMTV ORF 59R, Forward: GCATAGAGACGGATACAAGCG Reverse: GAAACAAGGCCGCTCTAGTC	Price et al.[1]	N/A
Primer: Major capsid protein gene (MCP) Forward: GTCCTTTAACACGGCATACCT Reverse: ATCGCT GGTGTTGCCTATC	Leung et al.[35]	N/A
Software and algorithms		
BioEdit version 7.2.6.	Hall[37]	https://thalljiscience.github.io
Mafft v7	Katoh et al.[38]	https://mafft.cbrc.jp/alignment/server/
JalView v2	Waterhouse et al.[39]	https://www.jalview.org
R	R Core Team[40]	https://www.R-project.org/
ape	Paradis et al.[41]	http://ape-package.ird.fr
ggtree	Yu et al.[42]	https://rdocumentation.org/packages/ggtree/versions/1.4.11
DnaSP v6.11.1	Rozas et al.[43]	http://www.ub.edu/dnasp/
BEAST v1.10.4	Suchard et al.[44]	https://beast.community

(*Continued on next page*)

Please cite this article in press as: Thumsová et al., Climate warming triggers the emergence of native viruses in Iberian amphibians, iScience (2022), https://doi.org/10.1016/j.isci.2022.105541

Continued

REAGENT or RESOURCE	SOURCE	IDENTIFIER
jModeltest	Darriba et al.[45]	https://github.com/ddarriba/jmodeltest2
Tracer v1.7.2	Rambaut et al.[46]	https://beast.community/tracer.html
FigTree v1.4.4	Rambaut[47]	https://github.com/rambaut/figtree/releases
ArcGIS v10.8	Esri	https://support.esri.com/en/products/desktop/arcgis-desktop/arcmap/10-8
JMP 16	SAS Inc.	https://www.jmp.com
Other		
MyGo Mini machine	IT-IS Life Science Inc.	http://mygopcr.com
GeneAmp PCR System 9700	Thermofisher Scientific Inc.	N/A

RESOURCE AVAILABILITY

Lead contact

Further information and requests for resources should be directed to and will be fulfilled by the lead contact, Jaime Bosch (jaime.bosch@csic.es).

Materials availability

This study did not generate new unique reagents.

Data and code availability

- All data are available in the figures, tables, and data files associated with this manuscript. Newly generated sequence data were deposited in GenBank. Accession numbers are listed in the key resources table and in Table S8.
- This study did not result in any unique code.
- Any additional information required to reanalyze the data reported in this paper is available from the lead contact upon request.

EXPERIMENTAL MODEL AND SUBJECT DETAILS

Sampling

We began amphibian disease surveillance in Spain in 1988 following the first mortality outbreak of *Alytes obstetricans* in the Pyrenees. That resulted in a long-term archive of carcasses preserved in 70% ethanol from multiple mortality events spanning 35 years. We thoroughly revisited this archive and sampled between one to three specimens exhibiting signs of ranavirosis, out of 15 never-before-studied mortality episodes.

METHOD DETAILS

DNA extraction and ranavirus detection

We performed DNA extractions from both liver tissue and toe/tail clips of every specimen using the DNAeasy Blood and Tissue kit (Qiagen GmbH, Hilden, Germany). We used a probe-based quantitative PCR (qPCR) assay specific to amphibian-associated ranaviruses to test all samples for the presence and quantification of ranavirus, targeting a 97 base pair region of the viral Major Capsid Protein gene (MCP[35]). We ran 20 μL reactions containing– 10 μL SensiFAST™ Probe No-ROX Kit (Meridian Bioscience Inc.), 5.95 μL nuclease-free water, 1 μL of each 10 μM stocks of forward (GTCCTTTAACACGGCATACCT) and reverse (ATCGCTGGTGTTGCCTATC) primers (0.5 μM final concentration), 0.05 μL of 100 μM stock of VIC-labelled probe (TTATAGTAGCCTRTGCGCTTGGCC; 0.25 μM final concentration), and 2 μL template DNA[35] with one no-template control and appropriate standards (extracted DNA from a *Common midwife toad virus* [CMTV] isolate,[1] using 0.1 mL MyGo mini tubes (IT-IS Life Science Inc.). By using a MyGo Mini machine (IT-IS Life Science Inc.) we conducted Real-Time PCR assays with the following cycle settings: 50°C for 2 min, 95°C for 10 min, and 50 cycles of 95°C for 15 s and 60°C for 30 s. We considered

Please cite this article in press as: Thumsová et al., Climate warming triggers the emergence of native viruses in Iberian amphibians, iScience (2022), https://doi.org/10.1016/j.isci.2022.105541

each sample as positive when both of the two duplicate analyses revealed infection loads >3 (the number of DNA copies presented in the smallest standard) and the amplification curves have a sigmoidal shape.

We subjected all positive tested samples to further PCR reactions to amplify the viral MCP gene using primers 4 and 5 from Mao et al.,[36] and the partial coding sequences from CMTV open reading frames 22L (GenBank: AFA_44926), 58L (GenBank: AFA_44964), 59R (GenBank: AFA_44965), 82L (GenBank: AFA_44988), and a region covering a noncoding sequence and the start of 13R (GenBank: AFA_44917). Firstly, we performed touchdown PCR technique[48] to amplify all products following the methods used in Price et al.[1] We ran reactions in individual 0.2 mL tubes in 15 μL total volumes comprising 7.5 μL GoTaq® Green Master Mix (Promega Biotech Inc.), 0.75 μL of 10 μM stocks of each primer, 4 μL of nuclease-free water, and 2 μL of template DNA. We set the initial annealing temperature several degrees above the calculated annealing temperature for the primers and then decreased by 0.5°C with each PCR cycle until it reached 50°C. We used Applied Biosystems Geneamp 9700 thermocycler to carry out touchdown PCR with the following cycle settings: a 10 min hold at 95°C to activate polymerase, 27 cycles of melting dsDNA at 95°C for 30 s, annealing primers at 63°C (decreasing to 50°C) for 30 s, elongating new DNA strands at 72°C for 25 s (small fragments) or 54 s (large fragments), then 15 additional, identical cycles with annealing temperature fixed at 50°C, before a five minute hold at 72°C to complete elongation and a hold at 4°C on completion. We stored all samples at 4°C prior to running on a 1.5% agarose gel stained with SYBR™ Safe DNA Gel Stain (Thermofisher Inc.) and with 100 base pair ladder as a size marker for at least 40 minutes (90V) to verify amplification success and confirm fragment size. To eliminate non-specific amplification of some samples, we carried out conventional PCR assays for each primer pair. In this case, we set the annealing temperature several degrees below the calculated annealing temperature for the primers. So, we ran the samples on the GeneAmp PCR System 9700 (Thermofisher Scientific Inc.) with the following settings for the viral MCP gene: 95°C for 10 min, followed by 35 cycles of denaturation at 95°C for 45 s, annealing at 52°C or for 45 s and extension at 72°C for 45 s, with a final 7 min extension step at 72°C before holding at 4°C.[20] To amplify the five additional loci (ORFs 13R, 22L, 58L, 59R, and 82L), we set the annealing temperature to 60°C. When amplification of non-specific products persisted, we increased the number of cycles to 45.

Sequencing and phylogenetics

We purified PCR amplicons and then submitted them to Macrogen Inc. (https://dna.macrogen.com) for Sanger sequencing of both DNA strands. We visually confirmed base calls by examining electropherograms in BioEdit version 7.2.6.[37] Then we viewed the aligned forward and reverse sequences for each sample and corrected ambiguous base calls with reference to the electrophoretograms of both sequences. We aligned sequences to published ranavirus sequences downloaded from the National Center for Biotechnology Information (NCBI) nucleotide database, using Mafft v7[38] with default settings (transition rate is twice the transversion rate, Gap opening penalty = 1.53). Alignments were converted between file formats using Prank v.140603. Alignments were trimmed and gaps and ambiguous base calls were removed manually in JalView v2.[39] To generate phylogenies, we concatenated alignments from individual loci using APE[41] in several combinations (as outlined in the main text) since we did not have a complete set of amplicons for all of the novel Spanish isolates nor other viruses of interest from the published literature. We used each concatenated alignment to construct phylogenetic trees using Bayesian analysis (MrBayes v3.2.1[49]; default settings used for Markov chain Monte Carlo (MCMC) — 2 runs with 4 chains each, 500,000 generations generally but 1 million generations where runs did not converge, sample frequency = 500, and a 25% burn-in).

To examine genetic diversity among ranaviruses further, we used two ranavirus sequence alignments to calculate matrices of pairwise genetic distances: 1) A partial MCP gene alignment, 2) A concatenated alignment of the 6 loci sequenced in this study which was trimmed to balance alignment length against the geographical coverage of isolates. The concatenated alignment contained fewer ranavirus isolates but had more sequence information than using MCP alone. To generate the MCP alignment, we used a BLAST search[50] of the NCBI nucleotide database to download MCP sequences for as many ranaviruses as possible. We combined the novel Spanish sequences (from this study) with the fasta outputs and trimmed them to the length of the shortest sequence. We aligned sequences and generated phylogenetic trees following the method described above. Trees are presented either as simple dendrograms with labelled tips or circular trees with tip labels replaced with coloured symbols, plotted with 'ggtree',[42] where size and colour are used to convey geographical information about where viruses were isolated. In order to

compare diversity among CMTVs by country of isolation, we identified CMTVs within our alignments by extracting the clade containing both CMTVs and FV3s and then excluding the FV3 clade, since CMTV did not resolve as a monophyletic group but FV3 always did in the relevant alignments used for these analyses. We calculated mean and maximum pairwise genetic distances within countries between CMTV ranavirus strains from around the world using both alignments, using the *dist.dna* function in the R package 'ape' using the Kimura's 2-parameter model of sequence evolution.[41] DNA polymorphism was analysed using DnaSP v6.11.1.[43] Five parameters including the number of polymorphic sites (S), the average number of differences (k), nucleotide diversity (π), Theta (θ)-W per sequence and Theta (θ)-W per site were estimated as the measurement of DNA polymorphism within populations (>2 isolates per country). To plot genetic distance against geographical difference we manually curated a database of locations of CMTV isolates (using the primary literature, our own previous studies and the isolates of this study).

Additionally, we used an alignment containing CMTV-like viruses to produce time-calibrated phylogeny with phylogeographical inference in the software BEAST v1.10.4.[44] Time and country of sampling were used as prior information. We applied a GTR substitution model, estimated in jModeltest[45,51] to best fit our data. Analyses were run for 200,000,000 generations logged every 20,000 generations. We set the substitution rate on 1.65×10^{-5} (1.6×10^{-5} to 1.9×10^{-6}) substitutions per site per year following estimates of Vilaça et al.[28] In Tracer v1.7.2[46] we checked effective sample size of >200. The sampled trees were combined into a single tree file with LogCombiner v1.10.4, discarding the first 20% of the trees. The maximum credibility trees were summarized using TreeAnnotator v1.10.4 and visualized in FigTree v1.4.4.[47]

QUANTIFICATION AND STATISTICAL ANALYSIS

We checked a possible shift in the temperature regimen preceding ranavirus outbreaks for every incident unequivocally attributed to a CMTV-like ranavirus by our phylogenetic analyses. First, we derived mean monthly temperatures for the period 1981–2020 at the exact place where each incident took place from projections based on data of Agencia Estatal de Meteorología of Spain (AEMET, http://www.aemet.es/es/serviciosclimaticos/datosclimatologicos). We used this data to generate yearly high-resolution maps (10 × 10 m), compiled and interpolated following Fries et al.[52] Then, we used a straightforward detrending technique by reducing all measurements to a reference level (ZDet) set to 1 masl (the lower boundary of the study area). We applied the respective altitudinal gradient for each pixel to reduce the measurements to the reference level altitude. We calculated the reference level of temperature by using the following equation:

$$TDet = T_{Month} + (\tau(Z_{Det} - Z_{Station}))$$

where T_{Month} is the average monthly temperature of each pixel, τ the altitudinal gradient calculated for each temperature, Z_{Det} the detrending level (here 1 masl) and $Z_{Station}$ the altitude of each sampling locality. After detrending, we converted these temperatures per 1 meter of altitude to a shapefile and interpolated by using ordinary kriging. In this system, we used 7 sampling localities to calculate the value of each pixel. The digital elevation model (DEM)[53] was used to re-establish the vertical temperature distribution for each pixel by inverting equation using the Spatial Analyst extension of ArcGIS v10.8:

$$T_{xy = T_{Det}} + \left(\tau * \left(Z_{(xy)} - Z_{Det}\right)\right)$$

where $T_{x,y}$ is the resulting monthly average temperature at a grid cell position x, y and $Z_{x,y}$ is the altitude of the DEM grid cell at position x, y [masl]. We used the Intersect tool for the extraction of mean temperature values, for each year, from the raster to each sampling point.

Finally, we used JMP 16 (SAS Inc.) to perform two separate regressions, one for before the year when the first mortality event was recorded, and one for after this year. Years were regressed against yearly averaged temperatures obtained as described before and the slopes of both models were compared by using a two-tail t-test. If the slopes did not statistically differ, we rescaled (centred) the independent variable (year) by subtracting the value of the first recorded mortality to check if the corresponding intercepts differed between the two models by using also a two-tail t-test.